Stem Cell Research 17 (2016) 413–421

Contents lists available at ScienceDirect

Stem Cell Research

journal homepage: www.elsevier.com/locate/scr

Metabolic switches during the first steps of adipogenic stem cells differentiation

Daiana Leila Drehmer [a], Alessandra Melo de Aguiar [a], Anna Paula Brandt [b], Lyvia Petiz [b], Sílvia Maria Suter Correia Cadena [b], Carmen K. Rebelatto [c], Paulo R.S. Brofman [c], Francisco Filipak Neto [b], Bruno Dallagiovanna [a], Ana Paula Ressetti Abud [a,*]

[a] Laboratório de Biologia Básica de Células Tronco, Instituto Carlos Chagas, Fiocruz, Curitiba, Paraná, Brazil
[b] Universidade Federal do Paraná, Paraná, Paraná, Brazil
[c] Pontifícia Universidade Católica do Paraná, Curitiba, Paraná, Brazil

ARTICLE INFO

Article history:
Received 4 January 2016
Received in revised form 30 August 2016
Accepted 2 September 2016
Available online 7 September 2016

Keywords:
Adult stem cells
Adipogenesis
Metabolism
Reactive oxygen species (ROS)
Antioxidant activity
Cytoprotection

ABSTRACT

The understanding of metabolism during cell proliferation and commitment provides a greater insight into the basic biology of cells, allowing future applications. Here we evaluated the energy and oxidative changes during the early adipogenic differentiation of human adipose tissue-derived stromal cells (hASCs). hASCs were maintained under differentiation conditions during 3 and 7 days. Oxygen consumption, mitochondrial mass and membrane potential, reactive oxygen species (ROS) generation, superoxide dismutase (SOD) and catalase activities, non-protein thiols (NPT) concentration and lipid peroxidation were analyzed. We observed that 7 days of adipogenic induction are required to stimulate cells to consume more oxygen and increase mitochondrial activity, indicating organelle maturation and a transition from glycolytic to oxidative energy metabolism. ROS production was only increased after 3 days and may be involved in the differentiation commitment. ROS source was not only the mitochondria and we suggest that NOX proteins are related to ROS generation and therefore adipogenic commitment. ROS production did not change after 7 days, but an increased activity of catalase and NPT concentration as well as a decreased lipid peroxidation were observed. Thus, a short period of differentiation induction is able to change the energetic and oxidative metabolic profile of hASCs and stimulate cytoprotection processes.

1. Introduction

Human adipose tissue-derived stromal cells (hASCs) are considered a potential source of adult stem cells (Gimble et al., 2007). hASCs can be easily isolated in large quantities with minimal invasion procedures (Zuk et al., 2002) and maintain the potential of differentiation into adipocytes. These features make these cells ideal candidates for use in cell therapy (Spangenberg et al., 2013). A better understanding of the specific mechanisms that regulate proliferation and differentiation of hASCs may yield information about how stem cells behave into an organism and suggest new strategies for therapy (Zhang et al., 2013).

Metabolism, mainly energy metabolism, plays an important role in dictating whether a cell proliferates, differentiates or remains quiescent and some metabolic pathways are known to determinate cell fate (Shyh-Chang et al., 2013). Metabolic modulation of adult stem cells can maintain stem cell potency (Zhang et al., 2013) or direct adult stem cell differentiation into specific cell types (Shyh-Chang et al., 2013).

In contrast to differentiated cells, stem cells appear to rely mainly on glycolysis to generate ATP (Rafalski et al., 2012). Studies analyzing energy metabolism of adult stem cells have focused on oxygen consumption (Pattappa et al., 2011) and mitochondrial activity (Zhang et al., 2013). Furthermore, there is an increased production of reactive oxygen species (ROS) as well as a dramatic change in antioxidant enzymes expression in differentiating cells (Rajasekhar and Vemuri, 2009). However, the metabolic changes that occur in early differentiation remain unclear. Knowledge of all steps of hASCs differentiation is essential to develop applications in regenerative medicine and tissue engineering, just as the understanding of the metabolism of embryos led to the development of in vitro fertilization during the 1960s (Shyh-Chang et al., 2013).

Here, we used adipogenic differentiation as a model to verify if a minimum period of differentiation induction is enough to change oxidative and energy metabolic profile. Knowledge of the adipogenic differentiation mechanisms is important to the discovery of new targets to treat obesity-related disorders (Liu et al., 2012). Adipogenesis is committed after three days of induction and gene expression analysis of this process shows differences in energetic metabolic profile after this short period, in comparison to control cells (Fig. 1) (Spangenberg et al., 2013). For this reason, we investigated mitochondrial activity, ROS generation and antioxidant systems during early adipogenic

* Corresponding author at: Instituto Carlos Chagas, Fundação Oswaldo Cruz – Paraná, Professor Algacyr Munhoz Mader Street, 3775, Curitiba 81350-010, Paraná, Brasil.
E-mail address: ana.abud@fiocruz.br (A.P.R. Abud).

http://dx.doi.org/10.1016/j.scr.2016.09.001

differentiation in order to understand the initial changes in cell metabolism that occur in response to the differentiation induction.

2. Materials and methods

2.1. Isolation, culture and differentiation of hASCs

hASCs, a fraction of which are stem cells, were obtained from adipose tissue from obese human donors. All samples were collected with previous consent, in accordance with the guidelines for research involving human subjects, and with the approval of the Ethics Committee of *Fundação Oswaldo Cruz*, Brazil (protocol 419/07). hASCs were isolated, cultured and characterized as previously described (Rebelatto et al., 2008). Briefly, 100 ml of adipose tissue was washed in sterile phosphate-buffered saline (PBS) (Gibco Invitrogen®). A one-step digestion by 1 $mg \cdot ml^{-1}$ collagenase type I (Invitrogen) was performed for 30 min at 37 °C during permanent shaking, followed by a filtration step through a 100 mesh filter (BD FALCON, BD Biosciences® Discovery Labware, Bedford, MA, USA). The cell suspension was centrifuged at 800*g* for 10 min, and erythrocytes were removed by lysis buffer, pH 7.3. The remaining cells were washed, filtered with a 40 μm mesh filter and then cultured at a density of 1×10^5 $cells \cdot cm^{-2}$ in T75 culture flasks with DMEM-F12 (Gibco Invitrogen®) supplemented with 10% FCS, penicillin (100 $units \cdot ml^{-1}$) and streptomycin (100 $\mu g \cdot ml^{-1}$) (routine medium). The culture medium was replaced 2 days after seeding, and then twice a week. hASCs were subcultured after reaching ≅80% confluence, utilizing 5 min trypsinization protocol (0.05% trypsin/0.02% EDTA, Invitrogen). Cell characterization was performed at passages 3 to 6 following the minimal criteria defined by Dominici et al. (2006). All tests were performed with cell cultures at passages 3 to 6. For adipogenic differentiation, hASCs were treated with inducing medium consisting of DMEM-F12 supplemented with 500 μM isobutylmethylxanthine (IBMX), 1 μM dexamethasone, 200 μM indomethacin and 1 $\mu g \cdot ml^{-1}$ insulin (all from Sigma Aldrich), during 3 or 7 days, with medium replacement every 3 or 4 days; controls were not treated with inducing medium. For the assays, cells were washed twice with a calcium- and magnesium-free buffered saline solution (CMF-BSS), and detached from the flasks with trypsin/EDTA.

2.2. Oxygen consumption

Mitochondrial respiration was determined by measuring mitochondrial oxygen consumption in a high resolution Oxygraph-2k (OROBOROS Instruments, Innsbruck, Austria) using two chambers at 37 °C under gentle agitation. DATLAB 4 software (OROBOROS Instruments) was used for data acquisition and analysis. Cell oxygen consumption rates were measured in DMEM medium (1×10^6 $cells \cdot ml^{-1}$) (basal state). Subsequent additions included sufficient oligomycin (2 $\mu g \cdot ml^{-1}$) to inhibit in situ mitochondrial ATP synthase and reflected the oxygen consumption due to mitochondrial proton leakage (leak state - the oxygen uptake in the presence of oligomycin results from the re-entry of protons into the mitochondrial matrix). After that, the mitochondrial uncoupler carbonylcyanide-4-(trifluoromethoxy)-phenylhydrazone (1 μM FCCP) was added to determine the maximal electron chain activity in mitochondria (uncoupled state - the addition of a classical uncoupler promotes a significant increase in oxygen consumption). The oxygen flow in these states was corrected by the subtraction of non-mitochondrial respiration, which

Fig. 1. GO analysis of two sets of differentially expressed genes. IN vs CT in the total RNA fraction (A) and IN vs CT in polysomal RNA (B). Data was analyzed with PANTHER classification system.

was obtained after addition of rotenone (1 μM) and antimycin (6 μg·ml^{-1}) (inhibited state) (Gnaiger, 2001; Scandurra and Gnaiger, 2009; Brandt et al., 2014). Results are expressed in pmol·s^{-1} (oxygen flux) per 1 × 10^6 cells.

2.3. Mitochondrial staining

Cells were washed in PBS and fixed with 4% paraformaldehyde. Mitochondria were stained with 100 nM MitoTracker Green FM (Life Technologies®) for 20 min at 37 °C, protected from light, and nuclei were labeled with 4′,6-diamino-2-phenyl-indole (DAPI, Invitrogen®). Cells were observed under Nikon Eclipse E600 fluorescence microscope. All images were taken using the microscope 40× objective and analyzed using ImageJ software.

2.4. Mitochondrial membrane potential

To evaluate mitochondrial membrane potential, cells were incubated with 100 nM MitoTracker Red (Life Technologies®) and 50 μM Rhodamine 123 (Life Technologies®), for 15 min at 4 °C (protected from light), washed and resuspended in PBS. Fluorescence intensity was measured on a FACSCanto flow cytometer (BD Biosciences, San Jose, CA) in 10^4 gated events and analyzed using FlowJo software.

2.5. Mitochondrial superoxide production

Cells were plated in UV-star microplates (Greiner - CELLSTAR®) and incubated with 50 μM MitoSOX Red (Molecular Probes®) for 10 min at 37 °C (protected from light), washed and resuspended in PBS. Fluorescence intensity was determined at 510 nm excitation/580 nm emission wavelengths on a microplate reader (BioTek®).

2.6. ROS/hydrogen peroxide detection

Cells were incubated with 35 μM 2′,7′-dichlorofluorescin diacetate (DCFH-DA) for 5 min at 37 °C (protected from light), washed and resuspended in PBS, as described by Eruslanov and Kusmartsev (2010). Fluorescence intensity was measured on a FACSCanto flow cytometer (BD Biosciences, San Jose, CA) in 10^4 gated events and analyzed using FlowJo software. This method is not entirely specific for hydrogen peroxide, but as it is the main ROS involved in the conversion of DCFH-DA to fluorescent 2′,7′-dichlorofluorescein (DCF), we refer to this method herein as hydrogen peroxide detection.

2.7. NADPH oxidase inhibition

To evaluate the NADPH oxidase role in ROS production in early differentiation, cells were incubated with apocynin (Sigma-Aldrich®), a NADPH oxidase inhibitor (Sun et al., 2015). Routine medium and differentiation medium were supplemented with apocynin (100 μM and 600 μM), added to cells and maintained during 3 days; DMSO was used as a negative control. After that, cells were processed for ROS detection analysis, as described in the item 2.6. Fluorescence intensity was measured on a FACSCanto flow cytometer (BD Biosciences, San Jose, CA) in 10^4 gated events and analyzed using FlowJo software. Mean ± SEM *$p < 0.05$.

2.8. Non-protein thiols concentration

Cells were washed twice in PBS, centrifuged at 300*g* and suspended in ice-cold lysis buffer (15 mM Tris–HCl, 15 mM $MgCl_2$, 300 mM NaCl, 1% Triton X-100; pH 7.4) for 10 min (5 × 10^5 cells·ml^{-1}). Cell lysate was centrifuged at 12,000 *g* for 10 min and the supernatant was used to determine non-protein thiols (NPT) concentration, represented mainly by glutathione (GSH). An aliquot (150 μl) of the supernatant was added to the reaction medium (25 μl of 3 mM DTNB [5,5′-dithiobis-(2-nitrobenzoic acid)] plus 125 μl of methanol) and absorbance was determined at 412 nm on a microplate reader (BioTek®). NPT concentration was calculated using the molar extinction coefficient of DTNB (ε = 13,600 M^{-1}·cm^{-1}). Results are expressed in μM -SH per 5 × 10^5 cells.

2.9. Catalase activity

Cells were washed twice in PBS, centrifuged at 720*g* and homogenized in ice-cold buffer (20 mM Tris–HCl, 1 mM EDTA, 1 mM PMSF; pH 7.6) and sonicated for 30 min at 4 °C. Cell lysate was centrifuged at 12,000 *g* for 30 min and an aliquot of the supernatant was used to determine the concentration of total proteins using the bicinchoninic acid assay, as described by Smith et al. (1985). For catalase activity, 50 μl of the supernatant was added onto UV-star microplates (Greiner - CELLSTAR®), followed by 200 μl of reaction medium (30 mM H_2O_2; 50 mM Tris-HCl; 0.25 mM EDTA; pH 8.0; 37 °C). Absorbance decrease was immediately measured at 240 nm and 25 s intervals during 6,25 min (25 cycles) on a spectrophotometer (ULTROSPECT 4300 PRO). Enzyme activity was calculated using the molar extinction coefficient of H_2O_2 (ε = 40 M^{-1} cm^{-1}). Results are expressed in mmol H_2O_2 degraded x min^{-1} × 10^6 cells.

2.10. Superoxide dismutase

Superoxide dismutase (SOD) activity was determined as described by Kono (1978). Cells were washed twice in PBS, centrifuged at 720*g* and homogenized in ice-cold buffer (20 mM Tris-HCl; 1 mM EDTA; 1 mM PMSF; pH 7.6). Cell lysate was centrifuged at 12,000*g* for 20 min, 150 μl of supernatant was mixed with 50 μl of ethanol and a new centrifugation was performed in the same conditions. Clear supernatant (10 μl) was added onto a 96-well microplate, followed by 70 μl of 100 μM nitroblue tetrazolium (prepared in 0.05 mM EDTA) and 120 μl of 36.85 mM hydroxylamine sulfate (prepared in 182 mM sodium carbonate buffer, pH 10.2). Absorbance increase was measured at 560 nm and 30 s intervals during 30 min on a microplate reader (BioTek®). Results are expressed in Units × min^{-1} × 10^{-6} cells.

2.11. Lipid peroxidation

Lipid peroxidation was determined using diphenyl-1-pyrenylphosphine (DPPP) (Okimoto et al., 2000). Cells were plated in UV-star microplates (Greiner - CELLSTAR®) and incubated with 50 μM DPPP for 15 min at 37 °C (protected from light) and washed twice in PBS. Fluorescence was determined at 351 nm excitation/380 nm emission wavelengths on a microplate reader (BioTek®).

2.12. Statistical analysis

Statistical procedures were performed in data obtained from at least three independent experiments carried out with hASCs from three different donors in biological replicates. Results are presented as mean ± SEM. The significance of the differences observed was evaluated by ANOVA, with Tukey's post hoc test. Values of $p < 0.05$ were considered as statistically significant.

3. Results

3.1. A metabolic switch from glycolysis to oxidative phosphorylation occurs in early adipogenic differentiation

Oxidative phosphorylation (OXPHOS) was analyzed during the initial steps of adipogenesis in order to evaluate the metabolic switch that occurs during hASCs differentiation. All accepted protocols use at least three days of strong induction to promote differentiation into adipocytes (Spangenberg et al., 2013), so hASCs were incubated in the

presence of adipogenic induction medium for 3 and 7 days. All the experiments described were performed with at least three samples of hASCs from different donors, all used in early passages. After 3 days of in vitro differentiation, the cells did not display clear changes in phenotype or accumulation of lipids in the cytoplasm, however, the expression of key adipogenic genes, FABP4 and PPARγ, was detected (Supplementary Table 1). After 7 days there was already a discreet presence of lipids in the cells and we confirmed the expression of adipogenic genes by qPCR (Supplementary Figs. 1 and 2).

We first evaluated the oxygen consumption rate by hASCs and only cells maintained for 7 days of induction presented an increase in oxygen consumption in the basal state (oxygen consumption in the absence of inhibitors or uncouplers), when compared to the control (Fig. 2B); 3-day induction had no effect on this parameter (Fig. 2A). So, mitochondrial mass and membrane potential were assessed. Mitochondrial mass was not altered after 3 and 7-day differentiation induction (Fig. 3A), but there was an increase in mitochondrial membrane potential after 7 days (Fig. 3B and C). By this result, we can say that mitochondria became more active with 7 days of induction, and probably these cells are synthetizing ATP preferentially through OXPHOS instead of glycolysis. These results also show that cells alter their gene expression after a short period of induction, but the phenotypic changes only occur with a longer stimulus time.

3.2. ROS production is increased in the first days of induction, but mitochondria were not the source

Cells induced for 3 days presented a higher production of hydrogen peroxide (Fig. 4). ROS production could be determining in cell commitment to adipogenic differentiation, as previous studies showed (Liu et al., 2012; Zhou et al., 2014; Wang and Hai, 2015). In addition, ROS source seems not to be mitochondria, since mitochondrial activity was similar to controls after 3 days of induction (Fig. 3C), and there was no increase in mitochondrial superoxide anion production at the same time point (Fig. 6A).

3.3. NADPH oxidase could be a ROS source in early differentiation

We asked if the ROS source in the first days of induction could be the NADPH oxidase family of proteins. For that, apocynin, an inhibitor of NADPH oxidase, was used to verify alterations in ROS production by hASCs after 3 days of adipogenic induction. We did not observe differences in ROS generation in the apocynin concentrations that were used (100 μM and 600 μM), as shown in Fig. 5. Given that in the absence of the inhibitor ROS was increased (Fig. 4), our results demonstrate a relation between ROS generation in the first days of induction and NADPH oxidase, and can indicate a role of these proteins in the commitment to adipogenic differentiation.

3.4. Antioxidant defenses change with hASCs adipogenic differentiation

Superoxide production was increased after 7 days of induction (Fig. 6A) and hydrogen peroxide levels were altered after 3-day, but not 7-day induction (Fig. 4). Mitochondria are the major source of intracellular ROS (Zhou et al., 2014) and it is possible that hydrogen peroxide had induced the antioxidant defense system after 3-day differentiation induction, so this system could avoid ROS accumulation during differentiation. To test this hypothesis, we evaluated the non-protein thiols (NPT) concentration (represented mainly by GSH), and the SOD and catalase activities, since these antioxidants provide the first line of defense against ROS. NPT concentration decreased after 3 (Spangenberg et al., 2013) and 7 days of induction, indicating redox challenge to cells and a cytoprotective response during differentiation (Fig. 6B). Likewise, SOD activity was increased since the first days of adipogenic differentiation (Fig. 6C). However, increase in catalase activity only occurred later, i.e. after 7 days of induction (Fig. 6D).

Like NPT, lipid peroxidation decreased after induction (Fig. 6E), which makes sense as GSH is required for detoxification of hydroperoxides generated by oxidative damage to lipids (Maddaiah, 1990).

4. Discussion

Studies with hASCs have demonstrated that careful manipulation of oxidative metabolism can direct the differentiation of these cells into adipocytes (Shyh-Chang et al., 2013). Thus, knowledge of all stages of differentiation of these cells, since the first days of induction, is of utmost importance to allow future applications. In this work, we used adipogenesis as a model in order to evaluate the changes in energy metabolism and redox milieu that occur in response to the early differentiation process. Adipogenic differentiation of hASCs is a complex phenomenon regulated on multiple levels and it is largely studied for the development of new targets to treat obesity-related disorders, for example (Wang and Hai, 2015).

Previous studies assessing stem cell metabolism during differentiation have focused on glucose consumption and lactate production (Pattappa et al., 2011) and demonstrated that adult stem cells use glycolytic metabolism as the main pathway to synthesize ATP (Rafalski et al., 2012). During adipogenic differentiation of hASCs, investigations about oxygen consumption have shown that it is increased when compared to undifferentiated control cells (Von Heimburg et al., 2005; Zhang et al.,

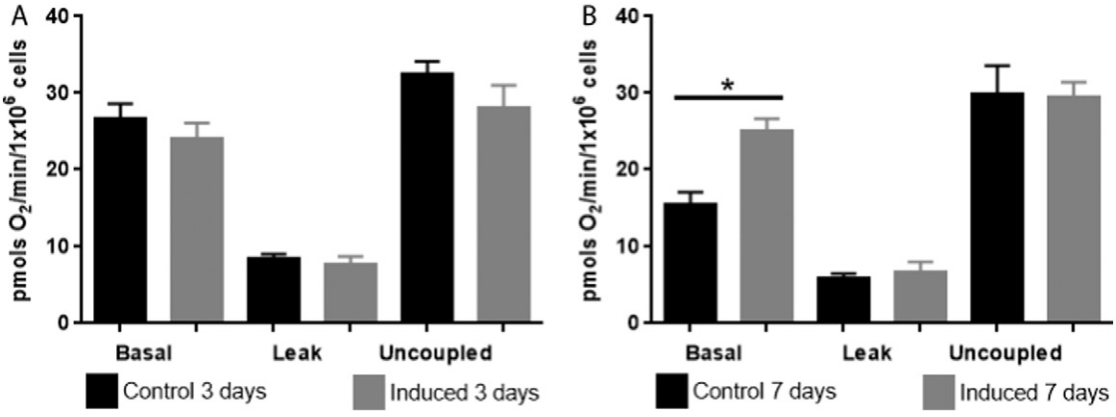

Fig. 2. Oxygen consumption using Oxygraph-2k. Quantitative comparisons of oxygen consumption rate in response to differentiation stimulus. Cells were maintained in differentiation-inducing conditions for three (A) and seven days (B). The oxygen consumption was rated in the different states of respiration that were defined as: basal state - oxygen consumption in the absence of inhibitors or uncouplers; leak state - the oxygen uptake in the presence of oligomycin results from the re-entry of protons into the mitochondrial matrix; uncoupled state - the addition of a classical uncoupler promotes a significant increase in oxygen consumption; inhibited state - non-mitochondrial respiration, which was obtained after addition of inhibitors. Means ± SEM *$p < 0.05$.

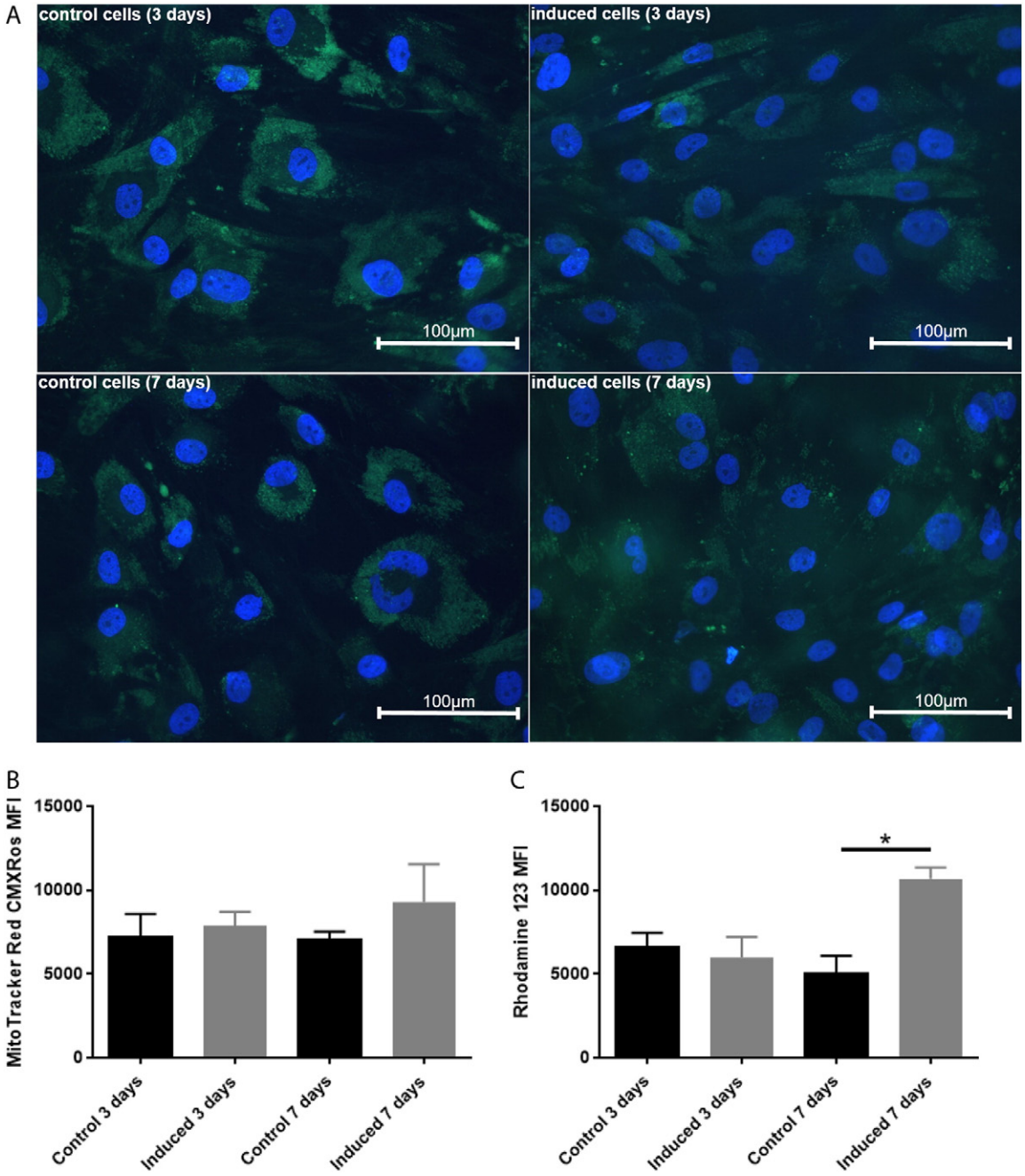

Fig. 3. Mitochondrial mass and activity analysis of hASCs. MitoTracker Green FM probe (Molecular Probes®) labelling (A). MitoTracker® Red CMXRos (Molecular Probes®) (B) and Rhodamine 123, FluoroPure™ grade (Molecular Probes®) (C). Mean fluorescence intensity distributions (MFI). Means ± SEM *$p < 0.05$.

2013). Unlike the previous studies, our work provides an assessment of the oxygen consumption by cells during the first days of differentiation.

We observed that 3 days of induction to adipogenic differentiation is not enough to change the oxygen consumption by hASCs. However, in 7 days of induction, the oxygen consumption is elevated in the basal state. Moreover, we assessed maximal oxygen consumption with the mitochondrial uncoupler FCCP (Zhang et al., 2013). Upon adipogenic differentiation, hASCs exhibited the same FCCP response that undifferentiated cells, suggesting that they still had not acquired maximum oxygen intake capacity. Our results also show that cells behave differently after maintenance in culture for different times. By comparing the control groups, differences in the basal oxygen consumption rate after 3 and 7 days are observed.

Recent discoveries have suggested crucial roles of mitochondria in the maintenance of potency and cell differentiation (Xu et al., 2013). Mitochondrial mass did not undergo changes with the induction stimulus for 3 and 7 days, but the organelle activity was increased after 7 days of differentiation, which can be related to the oxygen consumption rate. Thus, there is a switch from glycolytic metabolism to oxidative metabolism after 7 days of induction, and the cells begin to display higher mitochondrial activity, increasing OXPHOS. Gene expression analysis (Spangenberg et al., 2013) (Fig. 1) showed a transition from glycolytic to oxidative metabolism energy after induction for three days, but we observed that more time is needed to detect switches in cell phenotype.

Many authors suggest that an increased production of ROS in the beginning of differentiation is an essential factor for adipogenesis (Liu et al., 2012; Zhou et al., 2014; Wang and Hai, 2015). ROS could, in small quantities, act in cell signaling (Mc Bride et al., 2006; Zhang and Gutterman, 2007) and influence the function of several proteins involved in adipogenesis (Lowe et al., 2011). One of the reasons for that

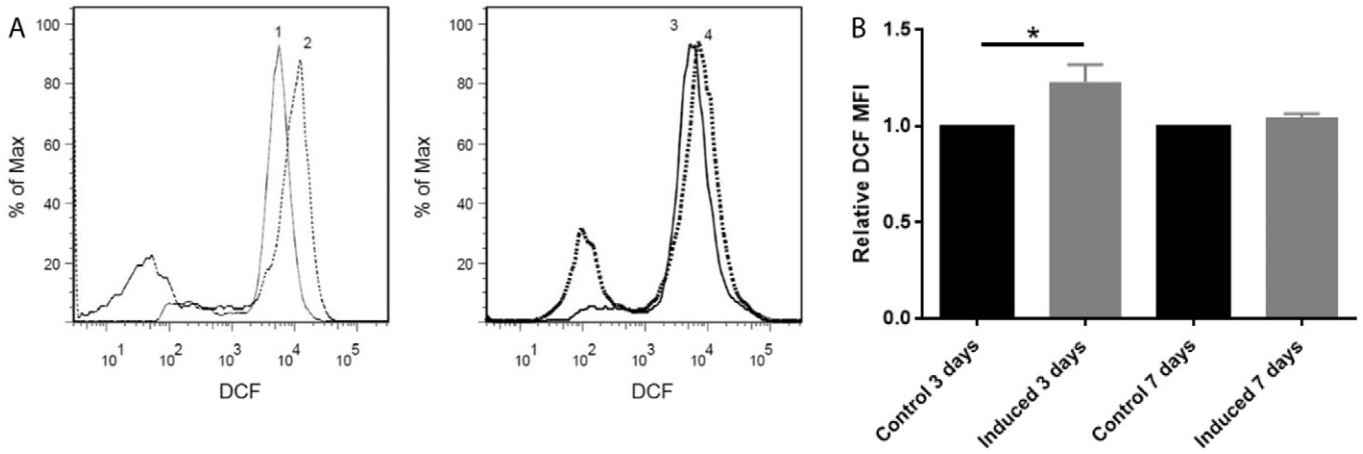

Fig. 4. Reactive oxygen species production. Histograms comparing fluorescence intensity of hASCs incubated with dichloro-dihydro-fluorescein diacetate (DCFH-DA) (Sigma-Aldrich®). Groups 1 and 2 (control and cells induced for three days) and 3 and 4 (control and cells induced for seven days) (A). Mean fluorescence intensity distributions (MFI) of hASCs incubated DCFH-DA (B). Mean ± SEM *$p < 0.05$.

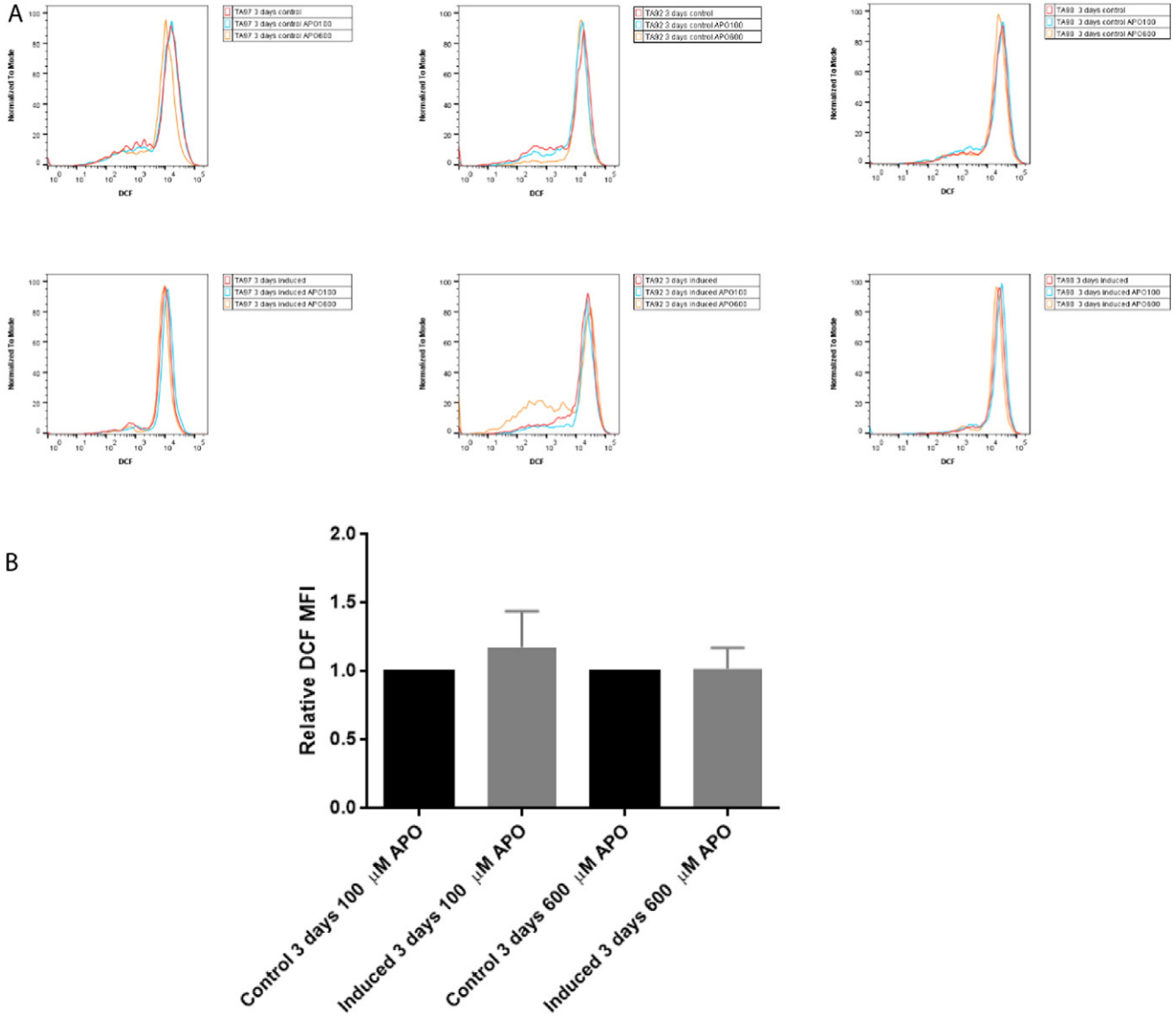

Fig. 5. Reactive oxygen species production after NADPH oxidase inhibition. Histograms comparing fluorescence intensity of hASCs treated with apocynin (100 µM and 600 µM) and incubated with dichloro-dihydro-fluorescein diacetate (DCFH-DA) (Sigma-Aldrich®) (A). Mean fluorescence intensity distributions (MFI) of hASCs incubated DCFH-DA (B). Mean ± SEM *$p < 0.05$.

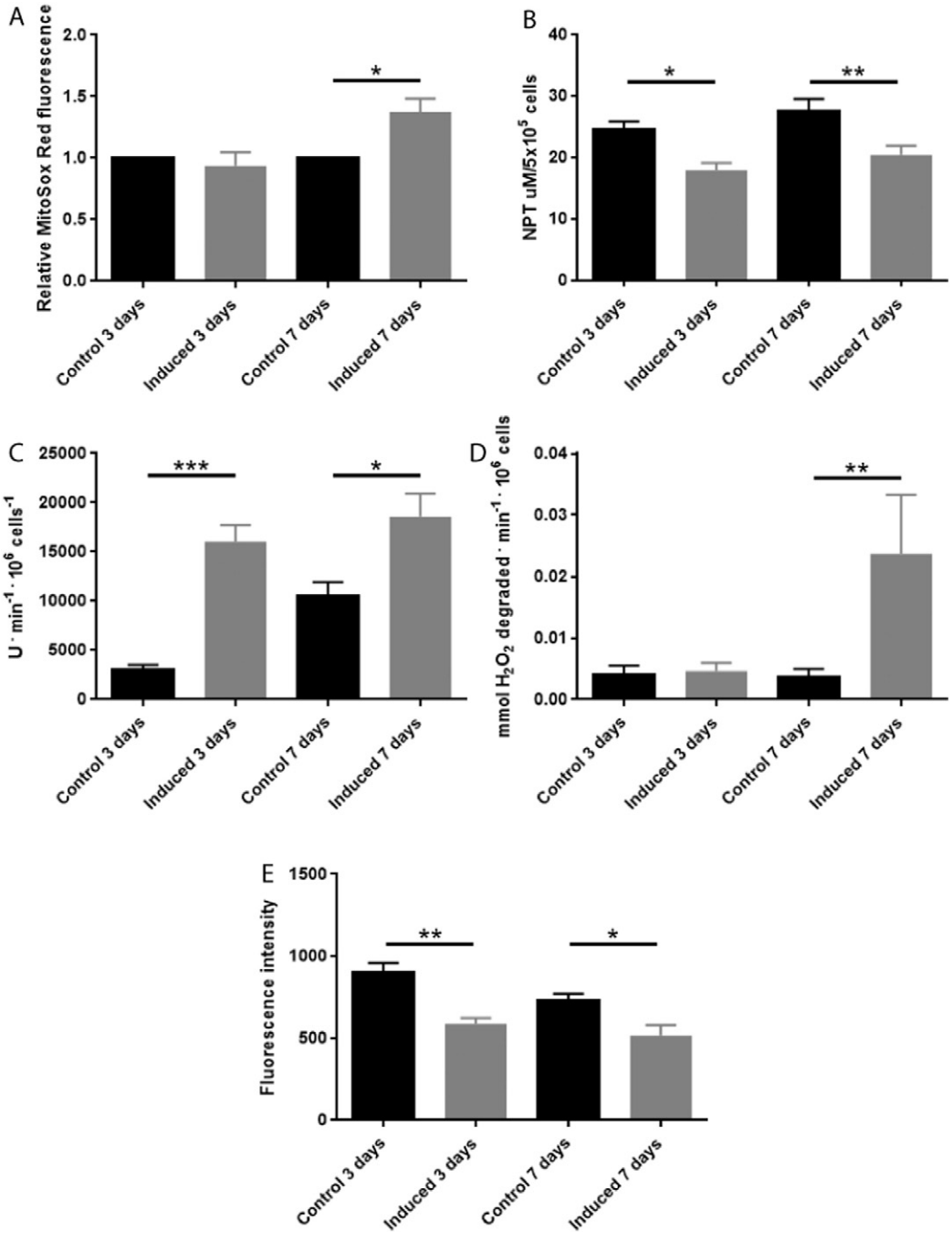

Fig. 6. Antioxidant activity. A - superoxide generation in mitochondria. Relative fluorescence intensity of hASCs incubated with MitoSOX Red (Molecular Probes®); B - Non-protein thiols (NPT) concentration; C - SOD activity; D - catalase activity; E - lipid peroxidation. Means ± SEM *p < 0.05, **p < 0.01. **p < 0.01, ***p < 0.001.

could be the suppression of pathways involved on osteoblast differentiation (Atashi et al., 2015). Mitochondria are the major source of intracellular ROS as a result of mitochondrial ETC activity (Zhou et al., 2014) and here we observed an increased mitochondrial activity in 7 days of adipogenic differentiation. We also analyzed ROS production by cells and, surprisingly, an increased production of ROS (hydrogen peroxide) was only detected in 3 days of induction, which may represent a stimulus for differentiation and can be related to cell commitment to adipogenesis. For 7 days of induction, however, ROS levels were the same as in the control group, showing that the antioxidant defenses were possibly stimulated in the cell.

Thus, the presence of ROS is important in the first steps of adipogenesis, but not in excess, since high concentrations may result in oxidative stress and cell damage. Here we only detected ROS in the first days of stimulus, followed by a return to control levels, indicating a cytoprotective activity. To confirm this hypothesis, we evaluated the NPT/GSH concentration and SOD and catalase activities, three essential antioxidants for redox milieu regulation (Zhou et al., 2014). The NPT concentration was lower for the induced cells (3 and 7 days), indicating the presence of high levels of ROS and oxidative stress (Spangenberg et al., 2013). SOD activity was significantly higher in induced cells, since the first days of differentiation, but catalase (CAT) activity was increased only after 7 days of induction. The SOD-CAT system usually work together, with SOD converting superoxide in hydrogen peroxide and CAT degrading it to water and molecular oxygen. SOD is widely distributed in cell compartments, but catalase is mainly peroxisomal in mammals (Glorieux et al., 2015). Thus, the increase of catalase activity and decrease of hydrogen peroxide after 7 days of induction is a preliminary

evidence of the involvement of peroxisomes in ROS production and in the process of differentiation into adipocytes. Lipid peroxidation can be initiated by hydroxyl radicals produced through Fenton and Harber-Weiss reactions (Das et al., 2015). Considering that lipid peroxidation decreased after 3 and 7 days of induction, efficient cytoprotective activity acted shortly after the differentiation stimulus initiation. In cells, the threshold between physiological/signaling levels of ROS and pathological ones is an increase in lipid oxidation (Singh et al., 2015). Thus, ROS produced in the first steps of differentiation may be at a signaling level.

ROS required for the commitment of differentiation may have come from other sources that not mitochondria, such as NADPH oxidase (NOX) (Kanda et al., 2011) and peroxisomes, since we observed an increase in ROS production but not in mitochondrial activity and mitochondrial superoxide generation in early stages of differentiation. ROS, as second messengers, are predominantly generated by the NOX family of proteins in the form of superoxide, a short-lived type of ROS (Pendyala and Natarajan, 2010). Taken together, our data suggest that NOX could be the source of ROS after 3-day induction of differentiation; in addition, SOD activity was also increased at day 3. To test our hypothesis, we used apocynin (Sigma-Aldrich®) as a NADPH oxidase inhibitor (Sun et al., 2015) and we measured ROS generation using DCFH-DA, as previously described. Cells treated with apocynin and induced to differentiation did not show alteration in ROS generation at the same time point when compared to control cells (Fig. 5), supporting our idea. In summary, we believe that superoxide can be produced by NOX and converted to hydrogen peroxide by SOD, and these events are leading to cytoprotection mechanisms that act avoiding oxidative stress and ROS deleterious effects.

5. Conclusions

Seven days of induction to adipogenic differentiation promotes a transition from glycolytic metabolism to OXPHOS. During this period, induced cells showed an increment in oxygen consumption, suggesting a stimulus for oxidative phosphorylation in these cells. The NPT concentration in cells induced to differentiation is lower than in the control group and shows that conversion of hASCs into adipogenic cells promotes oxidative stress. The higher production of hydrogen peroxide by hASCs is only observed in 3 days of induction, and this increase can be related to the commitment of differentiation. ROS source in the beginning of adipogenic differentiation could not be the mitochondria and our results show that the NADPH oxidase family of proteins can be involved in this process. Hydrogen peroxide production by cells induced for 7 days did not change when compared to the control, demonstrating that this time is necessary for an upregulation of antioxidant enzymes, such as catalase. In summary, a short period of differentiation induction is able to change the energetic and oxidative metabolic profile of these cells as well as stimulate cytoprotection processes (Fig. 7).

Supplementary data to this article can be found online at http://dx.doi.org/10.1016/j.scr.2016.09.001.

Conflict of interest

The authors declare that they have no conflicts of interest with the contents of this article.

Author contributions

DLD performed the assays, analyzed the data and drafted the article; AMA analyzed and helped in interpretation of results shown in Figs. 4 and 5; APB performed and analyzed the data shown in Fig. 2, LP performed the experiments shown in Fig. 2, SMSCC, FFN and BDM suggested assays, helped in results interpretation and drafted the article. hASCs were isolated and characterized by CKR and PRSB, APRA contributed for the conception and design, analysis, interpretation of data and drafting the manuscript. All authors approved the final version of the manuscript.

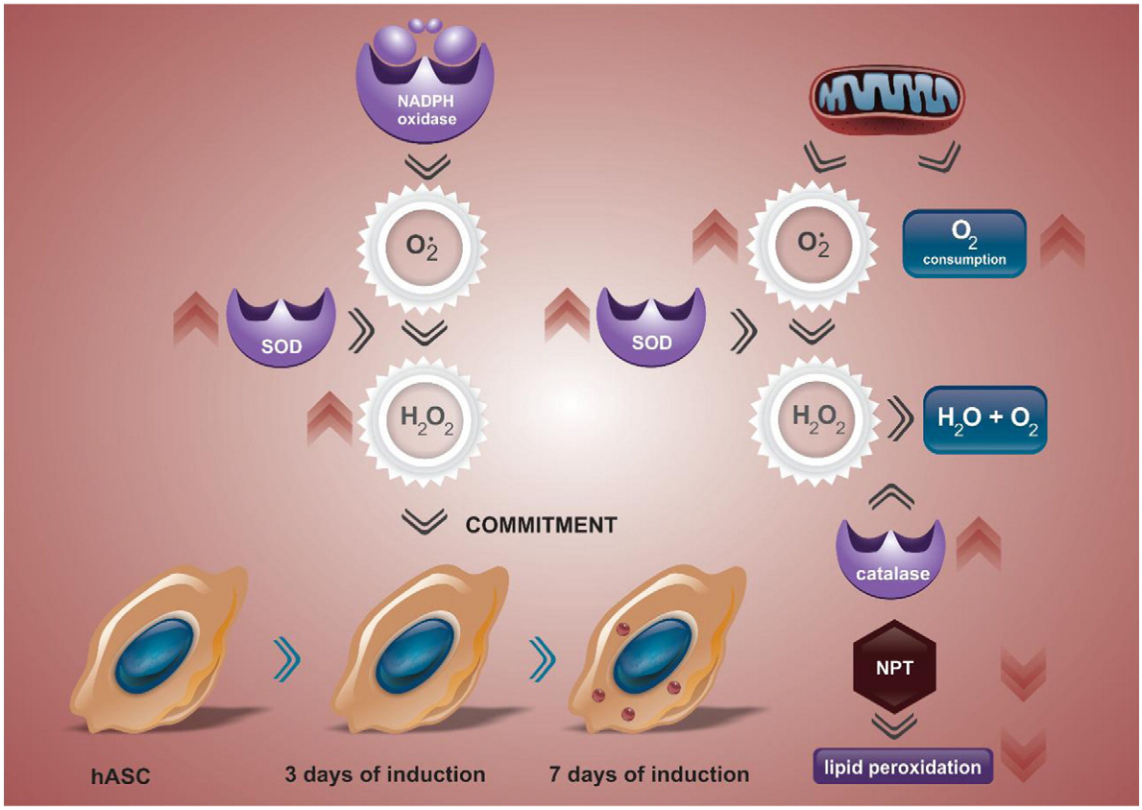

Fig. 7. Schematic design showing alterations that occur in the first days of adipogenic differentiation.

Acknowledgments

This work was supported by grants from Conselho Nacional de Desenvolvimento Cientifico e Tecnológico - CNPq (agreement 447149/2014-8)., A.P.R.A. received fellowship from Coordenação de Aperfeiçoamento de Pessoal de Nível Superior - CAPES/SETI/Fundação Araucária (agreement 1041/2013). The publication cost was provided by Fundação Araucária (agreement 1273/2012).

We would like to thank Dr. Carolina Camargo de Oliveira for providing us with the DCFH-DA probe, Dr. Ariel Silber for co-operation and stimulating discussions and supplying us with the Rhodamine 123 and MitoTracker Red CMXRos probes, Dr. Lysangela Alves for giving us the MitoTracker Green FM probe, Dr. Alexandre Costa for co-operation and helpful discussions, Dr. Alejandro Correa and Dr. Marco Stimamiglio for helpful discussions, Dr. Patrícia Shigunov, Msc. Isabela Tiemy Pereira, Msc. Bruna Marcon, Crisciele Kuligovski, Msc. Priscila Hiraiwa and Paulo Moro for scientific advice and technical support and Wagner Nagib de Souza Birbeire for graphic design.

References

Atashi, F., Modarressi, A., Pepper, M.S., 2015. The role of reactive oxygen species in mesenchymal stem cell adipogenic and osteogenic differentiation: a review. Stem Cells Dev. 24, 1150–1163.

Brandt, A.P., Andrade, Pires, A.R., Rocha, M.E.M., Noleto, G.R., Acco, A., De Souza, C.E.A., Echevarria, A., Canuto, A.V.S., Cadena, S.M.S.C., 2014. Sydnone SYD-1 affects the metabolic functions of isolated rat hepatocytes. Chem. Biol. Interact. 218, 107–114.

Das, T.K., Wati, M.R., Fatima-Shad, K., 2015. Oxidative stress gated by Fenton and Haber Weiss reactions and its association with Alzheimer's disease. Arch. Neurosci. 2, e20078.

Dominici, M., Le Blanc, K., Mueller, I., Slaper-Cortenbach, I., Marini, F., Krause, D., Deans, R., Keating, A., Prockop, D., Horwitz, E., 2006. Minimal criteria for defining multipotent mesenchymal stromal cells. The International Society for Cellular Therapy position statement. Cytotherapy 8, 315–317.

Eruslanov, E., Kusmartsev, S., 2010. In: Armstrong, D. (Ed.), Identification of ROS using oxidized DCFDA and flow-cytometry. Advanced Protocols in Oxidative Stress II, Methods in Molecular Biology 594, chapter 4. Humana Press, a part of Springer Science + Business Media, pp. 57–70.

Gimble, J.M., Katz, A.J., Bunnell, B.A., 2007. Adipose-derived stem cells for regenerative medicine. Circ. Res. 100, 1249–1260.

Glorieux, C., Zamocky, M., Sandoval, J.M., Verrax, J., Calderon, J.B., 2015. Regulation of catalase expression in healthy and cancerous cells. Free Radic. Biol. Med. 87, 84–97.

Gnaiger, E., 2001. Bioenergetics at low oxygen: dependence of respiration and phosphorylation on oxygen and adenosine diphosphate supply. Respir. Physiol. 128, 277–297.

Kanda, Y., Hinata, T., Kang, S.W., Watanabe, Y., 2011. Reactive oxygen species mediate adipocyte differentiation in mesenchymal stem cells. Life Sci. 89, 250–258.

Kono, Y., 1978. Generation of superoxide radical during autooxidation of hydroxylamine and an assay for superoxide dismutase. Arch. Biochem. Biophys. 186, 189–195.

Liu, G.S., Chan, E.C., Higuchi, M., Dusting, G.J., Jiang, F., 2012. Redox mechanisms in regulation of adipocyte differentiation: beyond a general stress response. Cell 1, 976–993.

Lowe, C.E., O'Rahilly, S., Rochford, J.J., 2011. Adipogenesis at a glance. J. Cell Sci. 124, 2681–2686.

Maddaiah, V.T., 1990. Glutathione correlates with lipid peroxidation in liver mitochondria of triiodothyronine-injected hypophysectomized rats. FASEB J. 4, 1513–1518.

Mc Bride, H.M., Neuspiel, M., Wasiak, S., 2006. Mitochondria: more than just a powerhouse. Curr. Biol. 16, 551–560.

Okimoto, I., Watanabe, A., Niki, E., Yamashita, T., Noguchi, N., 2000. A novel fluorescent probe diphenyl-1-pyrenylphosphine to follow lipid peroxidation in cell membranes. FEBS Lett. 474, 137–140.

Pattappa, G., Heywood, H.K., De Bruijn, J.D., Lee, D.A., 2011. The metabolism of human mesenchymal stem cells during proliferation and differentiation. J. Cell. Physiol. 226, 2562–2570.

Pendyala, S., Natarajan, V., 2010. Redox regulation of Nox proteins. Respir. Physiol. Neurobiol. 174, 265–271.

Rafalski, V.A., Mancini, E., Brunet, A., 2012. Energy metabolism and energy-sensing pathways in mammalian embryonic and adult stem cell fate. J. Cell Sci. 125, 5597–5608.

Rajasekhar, V.K., Vemuri, M.C., 2009. Regulatory Networks in Stem Cells. 1st ed. Human Press, New York.

Rebelatto, C.K., Aguiar, A.M., Moretão, M.P., Senegaglia, A.C., Hansen, P., Barchiki, F., Oliveira, J., Martins, J., Kuligovski, C., Mansur, F., Christofis, A., Amaral, V.F., Brofman, P.S., Goldenberg, S., Nakao, L.S., Correa, A., 2008. Dissimilar differentiation of mesenchymal stem cells from bone marrow, umbilical cord blood, and adipose tissue. Exp. Biol. Med. 233, 901–913.

Scandurra, F.M., Gnaiger, E., 2009. Cell respiration under hypoxia: facts and artefacts in mitochondrial oxygen kinetics. Adv. Exp. Med. Biol. 662, 7–25.

Shyh-Chang, N., Daley, G.Q., Lewis, C., Cantley, L.C., 2013. Stem cell metabolism in tissue development and aging. Development 140, 2535–2547.

Singh, M., Kapoor, A., Bhatnagar, A., 2015. Oxidative and reductive metabolism of lipid-peroxidation derived carbonyls. Chem. Biol. Interact. 234, 261–273.

Smith, P.K., Krohn, R.I., Hermanson, G.T., Mallia, A.K., Gartner, F.H., Provenzano, M.D., Fujimoto, E.K., Goeke, N.M., Olson, B.J., Klenk, D.C., 1985. Measurement of protein using bicinchoninic acid. Anal. Biochem. 150, 76–85.

Spangenberg, L., Shigunov, P., Abud, A.P.R., Cofré, A.R., Stimamiglio, M.A., Kuligovski, C., Zych, J., Schittini, A.V., Costa, A.D.T., Rebelatto, C.K., Brofman, P.R.S., Goldenberg, S., Correa, A., Naya, H., Dallagiovanna, B., 2013. Polysome profiling shows extensive posttranscriptional regulation during human adipocyte stem cell differentiation into adipocytes. Stem Cell Res. 11, 902–912 (Amsterdam. Print).

Sun, J., Ming, L., Shang, F., Shen, L., Chen, J., Jin, Y., 2015. Apocynin suppression of NADPH oxidase reverses the aging process in mesenchymal stem cells to promote osteogenesis and increase bone mass. Sci. Rep. 5.

Von Heimburg, D., Hemmrich, K., Zachariah, S., Staiger, H., Pallua, N., 2005. Oxygen consumption in undifferentiated versus differentiated adipogenic mesenchymal precursor cells. Respir. Physiol. Neurobiol. 146, 107–116.

Wang, X., Hai, C., 2015. Redox modulation of adipocyte differentiation: hypothesis of "Redox Chain" and novel insights into intervention of adipogenesis and obesity. Free Radic. Biol. Med. 89, 99–125.

Xu, X., Duan, S., Yi, F., Ocampo, A., Liu, G.-H., Belmonte, J.C.I., 2013. Mitochondrial regulation in pluripotent stem cells. Cell Metab. 18, 325–333.

Zhang, D.X., Gutterman, D.D., 2007. Mitochondrial reactive oxygen species-mediated signaling in endothelial cells. Am. J. Physiol. Heart Circ. Physiol. 292, 2023–2031.

Zhang, Y., Marsboom, G., Toth, P.T., Rehman, J., 2013. Mitochondrial respiration regulates adipogenic differentiation of human mesenchymal stem cells. PLoS One 8, 77077.

Zhou, D., Shao, L., Spitz, D.R., 2014. Reactive oxygen species in normal and tumor stem cells. Adv. Cancer Res. 122, 1–67.

Zuk, P.A., Zhu, M., Ashjian, P., Ugarte, D.A.D., Huang, J.I., Mizuno, H., Alfonso, Z., Fraser, J.K., Benhaim, P., Hedrick, M.H., 2002. Human adipose tissue is a source of multipotent stem cells. Mol. Biol. Cell 13, 4279–4295.